

Laser Welding-Brazing of Immiscible AZ31B Mg and Ti-6Al-4V Alloys Using an Electrodeposited Cu Interlayer

Zequn Zhang, Caiwang Tan, Gang Wang, Bo Chen, Xiaoguo Song, Hongyun Zhao, Liqun Li, and Jicai Feng

(Submitted June 26, 2017; in revised form January 4, 2018; published online January 30, 2018)

Metallurgical bonding between immiscible system AZ31B magnesium (Mg) and Ti-6Al-4V titanium (Ti) was achieved by adding Cu interlayer using laser welding-brazing process. Effect of the laser power on microstructure evolution and mechanical properties of Mg/Cu-coated Ti joints was studied. Visually acceptable joints were obtained at the range of 1300 to 1500 W. The brazed interface was divided into three parts due to temperature gradient: direct irradiation zone, intermediate zone and seam head zone. Ti₃Al phase was produced along the interface at the direct irradiation zone. Ti-Al reaction layer grew slightly with the increase in laser power. A small amount of Ti₂(Cu,Al) interfacial compounds formed at the intermediate zone and the (α-Mg + Mg₂Cu) eutectic structure dispersed in the fusion zone instead of gathering when increasing the laser power at this zone. At the seam head zone, Mg-Cu eutectic structure was produced in large quantities under all cases. Joint strength first increased and then decreased with the variation of the laser power. The maximum fracture load of Mg/Cu-coated Ti joint reached 2314 N at the laser power of 1300 W, representing 85.7% joint efficiency when compared with Mg base metal. All specimens fractured at the interface. The feature of fracture surface at the laser power of 1100 W was characterized by overall smooth surface. Obvious tear ridge and Ti₃Al particles were observed at the fracture surface with increase in laser power. It suggested atomic diffusion was accelerated with more heat input giving rise to the enhanced interfacial reaction and metallurgical bonding in direct irradiation zone, which determined the mechanical properties of the joint.

Keywords dissimilar joining, laser welded-brazed, magnesium alloy, microstructure, titanium alloy

1. Introduction

Recently, hybrid joints made of dissimilar materials have been attracting wide attention since they can overcome performance limitation of single materials. Magnesium and its alloys possess excellent properties, such as low density, high strength-to-weight ratio, good formability and easy recyclability. They have been widely utilized in the field of electronic communication, aerospace and automotive industry. Titanium alloys with a series of outstanding advantages, including

corrosion resistance, biocompatibility, high strength-to-weight ratio and high-temperature performance, offer dominant superiority in aerospace, defense and nuclear industries. Therefore, lightweight Mg/Ti hybrid structures are of great interest in weight reduction and increasing load capacity. Reliable and high-strength joining of Mg to Ti needs to be solved, which can in turn extend its engineering application in manufacturing industry.

However, there is no reaction or intersolubility between Mg and Ti according to the observation of Mg-Ti binary phase diagram. Hence, adding another intermediate element needs to be considered to realize metallurgical joining between Mg and Ti. The adopted element must react with or possess substantial solid solubility in both metals. Furthermore, the distinction in metallurgical and physical properties between Mg and Ti becomes an obstacle to join Mg/Ti. For instance, the boiling point of magnesium (1091 °C) is far lower than the melting point of titanium (1678 °C), suggesting conventional fusion welding does not work here.

Various welding techniques such as friction stir welding (FSW) (Ref 1, 2), tungsten inert gas (TIG) welding (Ref 3), cold metal transfer (CMT) welding (Ref 4), transient liquid phase (TLP) bonding (Ref 5-7) and laser welding (Ref 8-10) were employed to solve these challenges. Aonuma and Nakata (Ref 1) reported that Al alloying element from Mg base metal had an effect on FSW of Mg to Ti. TiAl₃ was observed at the joint interface. It was found that increased Al content increased the thickness of the TiAl₃ interfacial reaction layer and decreased tensile strength. Then, calcium (Ca) element added in Mg-Al alloy was adopted to improve joint strength by suppressing the formation of TiAl₃ intermetallic compound

Zequn Zhang, Caiwang Tan, and Xiaoguo Song, State Key Laboratory of Advanced Welding and Joining, Harbin Institute of Technology, Harbin 150001, China; and Shandong Provincial Key Laboratory of Special Welding Technology, Harbin Institute of Technology at Weihai, Weihai 264209, China; **Gang Wang**, State Key Laboratory of Advanced Welding and Joining, Harbin Institute of Technology, Harbin 150001, China; and School of Mechanical and Automotive Engineering, Anhui Polytechnic University, Wuhu 241000, China; **Bo Chen** and **Hongyun Zhao**, Shandong Provincial Key Laboratory of Special Welding Technology, Harbin Institute of Technology at Weihai, Weihai 264209, China; **Liqun Li** and **Jicai Feng**, State Key Laboratory of Advanced Welding and Joining, Harbin Institute of Technology, Harbin 150001, China. Contact e-mails: tancaiwang@163.com, xgsong@hitwh.edu.cn, and zhangzequncrystal@163.com.

owing to the reaction between Ca and Al (Ref 2). Xu et al. (Ref 3) investigated TIG welding-brazing of Mg to Ti assisted with ultrasonic vibration. Compared with that without ultrasonic vibration, equiaxed grains were obtained and joint strength improved by 18.1%. In the case of CMT welding-brazing process, the fracture load obtained by Mg-Ti joint (top Mg sheet-bottom Ti sheet) was superior to that of Ti-Mg joint (Ref 4). Ti_3Al , $Mg_{17}Al_{12}$ and $Mg_{0.97}Zn_{0.03}$ intermetallics composed brazing interface, which indicated Al element and Zn element from Mg base metal and Mg-based filler played an important role in joining Mg/Ti dissimilar metals. Anas et al. (Ref 5) used nickel (Ni) foil as an interlayer during semisolid TLP bonding of Mg to Ti. Reaction layers with different morphologies affected by bonding time and bonding temperature were found. After this, pure thin Ni electrodeposited coat layer was employed (Ref 7). The presence of Ni coating resulted in the formation of Mg_2Ni eutectic phase and some ternary phases (Mg_3AlNi_2 and Mg_3TiNi_2) at the interface. The joint width and size of phases and intermetallics had a crucial effect on shear strength. Then, they tried nanoparticle Ni or Cu dispersion used in Ni coating to join Ti alloy an Mg alloy (Ref 6). The result showed that the presence of nanoparticles within the joint region had a positive effect on joints formation. They concluded that nanoparticles would diffuse faster to parent alloy than bulk foil material and could promote the formation of eutectic structure at a lower temperature owing to possessing high surface to volume ratio.

When it comes to joining dissimilar metals, laser welding-brazing technique offers great advantages over conventional welding techniques in terms of flexibility. Dissimilar systems such as Al/steel (Ref 11-13), Al/Ti (Ref 14) and Mg/steel (Ref 15) were joined successfully by laser welding-brazing. Gao et al. (Ref 8) adopted laser keyhole welding to bond Mg/Ti alloy and focused on the effect of laser offset on bonding mechanism and joint properties. Laser offset played a crucial part on changing the power density which impacted on process stability and weld characterizations. Tan et al. (Ref 9) added Al alloying element from Mg-AZ91 (9% Al) filler to enhance interfacial reaction. Ti_3Al phases were observed along the interface. Afterward, Tan et al. (Ref 10) studied the effect of laser welding-brazing parameters on weld appearance and mechanical properties. The best performance of the joint was attained when laser power of 2400 W, welding speed of 0.5 mm/min and feed speed of 3.5 mm/min were employed. The joint reached the highest fracture load of 2057 N, reaching 50% joint efficiency referring to Mg base metal. All these results confirmed the feasibility of Al element in improving the interfacial reaction between Mg and Ti by laser welding-brazing process. However, the content of Al element was not easy to control on account of the limited amount Al added in Mg-based filler and difficulty in fabricating the filler. Therefore, electrodeposition was employed as a more convenient way to add alloying elements.

This work selected Cu element as an intermediate element to enhance interfacial joining and mechanical properties when bonding immiscible Mg and Ti because Cu can react with Mg or Ti and produce intermetallic compounds according to Mg-Cu (Ref 16) or Cu-Ti (Ref 17) binary phase diagram. Additionally, the Cu element was adopted only in the form of nanoparticles dispersed in the Ni coating when using TLP bonding by Atieh and Khan (Ref 6). Although the joint strength of Mg/Ni-coated Ti joint with Cu nanoparticles was higher than that without any nanoparticles, Cu nanoparticles were not

added in this work. Considering the characteristics of laser welding-brazing above and the effect of nanoparticles, the advantage of faster diffusion would not be significant because liquid state would form in a very short period of time. In this study, the objective is to study the effect of laser power on weld appearance, microstructure and mechanical properties. According to the analyses above, the bonding mechanism of Mg/Cu-coated Ti by laser welding-brazing process with AZ92 filler was elucidated.

2. Experimental Procedure

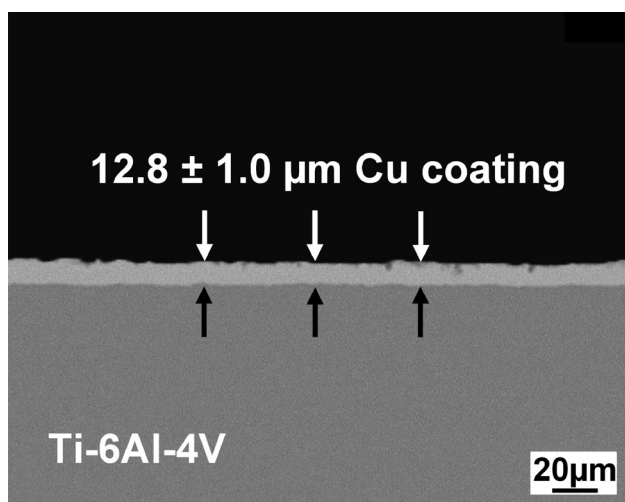
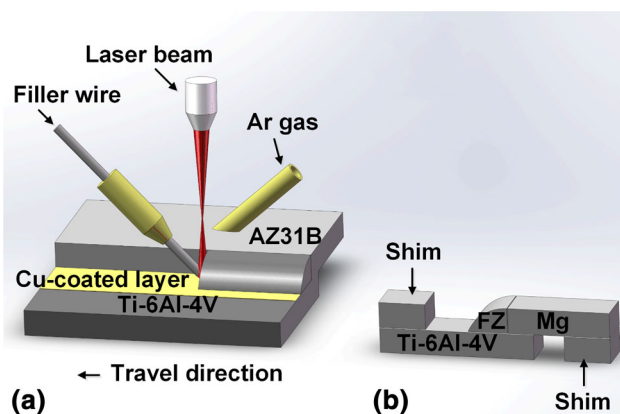
Mg-AZ31B alloy and Ti-6Al-4V alloy were adopted as base metals with the same dimension of $100 \times 55 \times 1.2$ mm. AZ92 (9% Al and 2% Zn) Mg-based filler with the diameter of 1.6 mm was employed. The chemical compositions of the base metals and filler metal are shown in Table 1. The surface of Ti alloy was pickled to remove the oxide film by the solution of an acid (15% HCl, 5% HF and 80% distilled water) for 3 min and then cleaned with tap water for 30 s. the electrodeposition of pure Cu coating was carried out immediately after preparing the specimen surface. 55 g $K_4P_2O_7 \cdot 3H_2O$, 5 g $C_6H_{17}N_3O_7$, 12 g $CuSO_4 \cdot 5H_2O$ and 6 g $Na_2HPO_4 \cdot 12H_2O$ were dissolved in 250 mL distilled water to prepare plating solution. The titanium sample and Cu sheet were set as cathode and anode, respectively. Current density was kept at $0.5 A/dm^2$, and the coating temperature was maintained at $35^\circ C$. The coating time was set up for 1 h with magnetic stirring of 200 revolutions per minute (RPM). Figure 1 shows the cross-sectional SEM micrograph of Cu-coated Ti-6Al-4V. A continuous and uniform pure Cu coating layer was observed on the titanium surface. And coating thickness approximately was $12.8 \pm 1.0 \mu m$.

Figure 2(a) is the illustration of the laser welding-brazing process. The lap configuration with Cu-coated Ti base metal placed under the bottom of Mg base metal was performed. A fiber laser (IPG YLR-6000) with the maximum power of 6 kW, wavelength of 1070 nm and beam parameter product of 7.2 mm mrad was used in experiment. The focused spot size of laser beam was 0.2 mm. The oxide layers on the surface of Mg sheets were removed by stainless steel wire brushing before laser welding-brazing process. Both specimens were put into acetone to clean up the surface. Laser vertical irradiation was performed on the Ti base metal behind the feeding of filler metal. The oxidation of molten pool was protected by argon gas with the flow rate of 20 L/min. The experiment was carried out with the process parameters as exhibited in Table 2.

Specimens were cut to prepare metallurgical examination and tensile test after welding-brazing process. Standard metallographic preparation procedures were utilized. The appearance, cross section, microstructure and fracture surface were observed using optical microscope (OM) and scanning electron microscope (SEM). The chemical composition of the interface was analyzed by energy-dispersive x-ray spectrometer (EDS). The phase characterization of the newly formed reaction products along the interface was conducted by micro-x-ray diffraction (XRD) analysis. Micro-Vickers hardness was measured under the test load of 100 g and dwell time of 10 s. The specimens used for tensile-shear testing were cut into 100 mm long and 10 mm wide pieces. Cross speed of 1 mm/min was adopted during tensile-shear testing process. An average of three measurements for fracture load was carried out via the test.

Table 1 Chemical compositions of base metals and filler metal (wt.%)

	Al	Zn	Mn	Fe	V	Si	Mg	Ti
AZ31B	2.5-3.5	0.5-1.5	0.2-0.5	<0.005	...	0.1	Bal.	...
Ti-6Al-4V	5.5-6.8	3.5-4.5	...	0.3	3.5-4.5	Bal.
Filler metal	8.3-9.7	1.7-2.3	0.15-0.5	<0.005	...	<0.05	Bal.	...

**Fig. 1** SEM image for cross section of Cu coating on Ti-6Al-4V substrate**Fig. 2** Schematic of laser welding-brazing of Mg to Cu-coated Ti: a laser welding-brazing process; b specimen for tensile-shear test**Table 2 Experimental parameters used in the process**

Welding parameters	Value
Laser power, W	1100-1900
Defocus distance from steel surface, mm	+ 20
Welding speed, m/min	0.5
Wire feed speed, m/min	2.5
Flow rate of shielding gas Ar, L/min	20

3. Result and Discussion

3.1 Joint Appearance and Cross Section

Figure 3 shows representative appearances of laser welded-brazed Mg/Cu-coated Ti joints welded with different laser

powers. Rough front surface appeared with the laser power of 1100 W as shown in Fig. 3(a). The back surface was not fully penetrated, which was caused by relatively lower heat input. In addition, high reflectivity of Cu coating on laser beam reduced incident light to a great extent, leaving only part of laser to irradiate filler wire and base metals. Satisfactory bead surface without visible defects was achieved when further increasing laser power to the range of 1300 to 1500 W, which was indicative of process stability in these cases. It was attributed to the improvement in wetting-spreading ability of molten filler on Cu-coated Ti surface with higher heat input. However, the bead shape became uneven and discontinuous with the laser power of 1700 W (Fig. 3d). Burning-through defect occurred with the increase in laser power to 1900 W, as indicated in Fig. 3(e). Severe evaporation of Mg fusion zone (FZ) would occur with the excessive laser power because of low boiling point of Mg alloy.

Figure 4 presents cross sections of laser welded-brazed Mg/Cu-coated Ti joints. Fusion zone took shape by mixing molten AZ92 filler and part of the Mg base metal, and brazed interface was produced between the molten filler and Ti sheet. Slight melting of Ti was noticed as laser power increased (Fig. 4), which was associated with locally high thermal gradient of laser welding characteristics. In addition, deeper penetration, larger seam width and smaller contact angle of the joints were obtained with the increase in laser power. The contact angle and seam width were measured to expound clearly the role of the laser power on the wetting and spreading ability of molten filler wire on the Cu-coated Ti. From the corresponding results shown in Fig. 5, the contact angle attained almost 45°, while the seam width was only 5.49 mm with the low laser power of 1100 W. As the laser power increased to 1300 W, the contact angle was less than 40° and the seam width reached 6.04 mm. These data indicated that suitable heat input was able to improve the spread of liquid filler on the Cu-coated Ti. The contact angle continued to reduce to approximately 20° and the seam wide increased to 8.24 mm with further increase the heat input. However, higher laser power resulting in evaporation of Mg-based filler metal shown in Fig. 3(d) manifested that excessive heat input was not appropriate in this work.

3.2 Interfacial Microstructure

The interfacial SEM morphologies of Mg/Cu-coated Ti joints with various laser power of 1100, 1300 and 1700 W are shown in Fig. 6, which was much different with the interfacial structure morphologies observed in the research of Atieh and Khan (Ref 6). The interfacial reaction layer was uniform and thin in TLP bonding, while various reaction products were found in this work. Based on the different positions of laser beam irradiation and distribution of reaction products, the interface was divided into three parts: direct irradiation zone, intermediate zone and seam head zone. The high temperature gradient characteristic of laser irradiation was mainly respon-

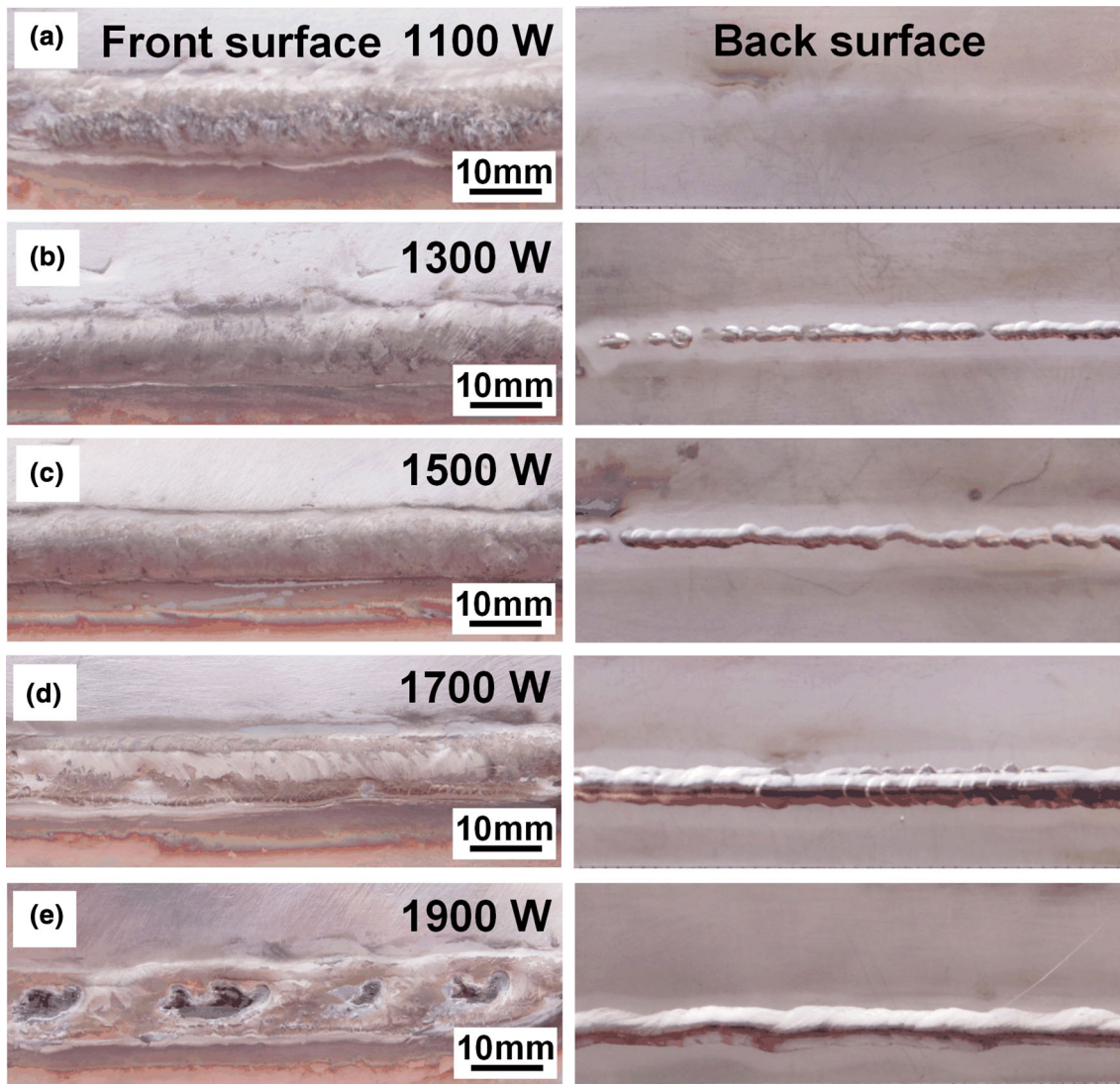


Fig. 3 Appearances of laser welded-brazed dissimilar Mg/Cu-coated Ti joints at different laser powers: (a) 1100 W, (b) 1300 W, (c) 1500 W, (d) 1700 W, (e) 1900 W

sible for this according to our previous study of Mg/steel (Ref 18).

Figure 6(a), (b) and (c) shows the SEM images of Mg/Cu-coated Ti joint produced at the laser power of 1100 W. In order to confirm the phase components and structure, relevant EDS analyses were performed and the results are shown in Table 3. No obvious reaction layer was observed at direct irradiation zone in Fig. 6(a). ESD line scanning was carried out to identify the concentration of element along the FZ/Cu-coated Ti interface at this zone. The corresponding result is shown in Fig. 7(a). Mg element decreased and Ti element increased gradually without significant concentration from the FZ to Ti substrate. There was no segregation of Cu element, suggesting that Cu coating totally melted under the action of high temperature. And then, Cu atoms dissolved into the molten pool to participate in microstructure development. Meanwhile, Al segregation was found, indicating that the diffusion of Al atoms occurred. Precipitated phase in the FZ indicated by arrowed line in Fig. 7(a) was the main reason for the higher content of Al element at the FZ. The EDS mapping was performed to further observe the representative segregation of

Mg, Al, Cu and Ti at the same zone. The distribution result (Fig. 8) verified the above analysis results. Combined with the results from previous study (Ref 9), the formation of Ti_3Al reaction layer was confirmed along the interface. EDS result showed that dark phase (P1) in the FZ mainly contained 96.58 at.% Mg and 3.42 at.% Ti, indicating P1 was α -Mg phase. EDS analysis result of gray dot phase (P2) mainly consisted of 82.03 at.% Mg and 17.08 at.% Al, which was confirmed as $Mg_{17}Al_{12}$ precipitated phase. This precipitated phase was produced during eutectic reaction, which was also observed in the study of Mg/Ti joining using TIG welding-brazing (Ref 19). In addition, some gray phase (P3) in large size distributed at the matrix of Mg solid solution. The particle was identified as $Mg_{17}(Al,Zn)_{12}$ intermetallic compound, which contained 76.62 at.% Mg, 20.40 at.% Al and 2.70 at.% Zn based on the EDS result. The replacement between Zn atoms and Al atoms was considered the main reason for the formation of P3. Similar phenomenon was reported both in the studies of Gao et al. (Ref 20) and Ma et al. (Ref 21). The magnified SEM of laser power on the interfacial lamellar shape microstructure (P4) adjacent to the Ti side shown in Fig. 5(a) was confirmed as

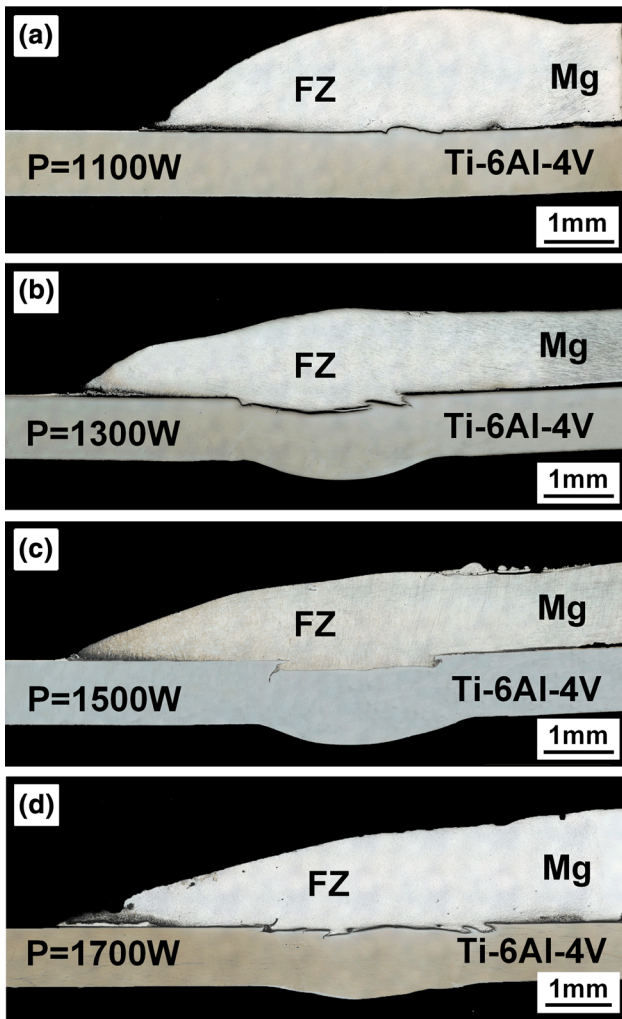


Fig. 4 Cross sections of laser welded-brazed dissimilar Mg/Cu-coated Ti joints at different laser powers: (a) 1100 W, (b) 1300 W, (c) 1500 W, (d) 1700 W

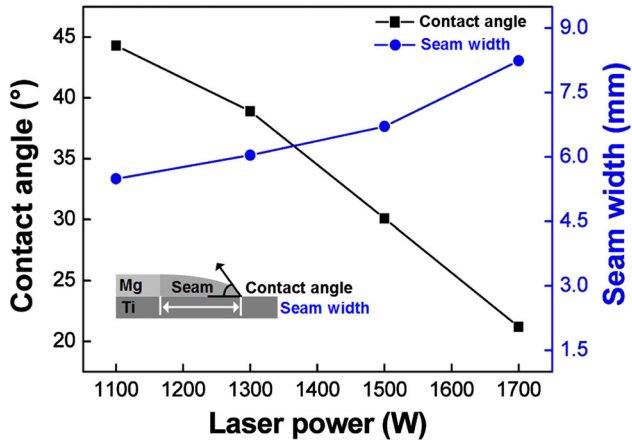


Fig. 5 Variation of contact angle and seam width of Mg/Cu-coated Ti joints as a function of laser power

(α -Mg + Mg₂Cu) eutectic structure since it consisted of 80.37 at.% Mg, 13.22 at.% Al and 6.41 at.% Cu. The result was in good agreement with the result obtained in Mg/Cu laser-

arc hybrid welded joint (Ref 22). A great number of Mg-Cu eutectic structures were found as shown in Fig. 6(b) and (c). A large amount of Cu coating was involved into the intermediate zone and seam head zone and induced reaction with Mg, which was attributed to the flow and vortex formed in the molten pool. Based on the EDS results, a lamellar microstructure (P5) containing 80.97 at.% Mg, 9.56 at.% Al and 9.48 at.% Cu was identified as (α -Mg + Mg₂Cu). Besides, some blocky particles (P6) were observed adjacent to the FZ/Ti interface. It was identified as Mg(Cu,Al)₂ since it was mainly composed of 34.82 at.% Mg, 22.18 at.% Al and 42.23 at.% Cu. The formation of this phase was associated with the eutectic reaction. MgCu₂ binary cubic phase was precipitated from the liquid with some Al atoms replacing Cu atoms, giving rise to the Mg(Cu,Al)₂ phase.

With further increase in the laser power to 1300 and 1700 W, more Mg₁₇Al₁₂ precipitated phase and less Mg-Cu eutectic phase adhering to the Mg/Ti interface were observed at the direct irradiation zone as exhibited in Fig. 6(d) and (g), respectively. It was because higher laser power induced more intense reaction between Mg element and Al element and more violent stirring of molten pool. Corresponding EDS line scanning results presented in Fig. 7(b) and (d) showed similar trend with that obtained with the laser power of 1100 W (Fig. 7a). However, the thickness of reaction layer grew from 2.29 to 3.40 μ m with the variation of laser power, which suggested that higher heat input was beneficial to the formation of Ti₃Al. Note that Ti-Al reaction layer grew slightly even at high laser power, which could be interpreted as limited content of Al element existed in Mg-based filler. The rapid heating and cooling rate of laser welding-brazing also restricted the mutual diffusion of Al atoms from the Mg-based filler and Ti atoms from the Ti substrate. In the study of Mg/steel joining with Mg-Al-Zn filler wire (Ref 12), similar phenomenon was reported. And the work reported that the thickness of the interfacial reaction layer below 10 μ m was beneficial to joint strength. Cu segregation presented in Fig. 7(d) was caused by the presence of (α -Mg + Mg₂Cu) eutectic structure adhering to the FZ/Ti interface. At the intermediate zone (Fig. 6e and h), the microstructure evolution was found to be significantly different from that with lower power of 1100 W (Fig. 6b). The Mg-Cu eutectic structure dispersed in the FZ instead of gathering near the interface (Fig. 6b). And ultra-thin and uneven reaction layer was observed from the magnified SEM morphology in the inset of Fig. 6(e). P7 was mainly composed of 10.09 at.% Al, 68.46 at.% Ti and 20.37 at.% Cu based on the EDS result presented in Table 3. In this phase, the atomic fraction of Ti/(Cu + Al) was approximately equal to the atomic fraction of Ti/Cu from Ti₂Cu. Therefore, P7 was identified as Ti₂(Cu,Al). Line scanning analysis result obtained at intermediate zone under the laser power of 1300 W is shown in Fig. 9. High segregation of Al and Cu was found, suggesting that Al atoms and Cu atoms diffused at the FZ/Ti interface. This finding was proved by element mapping shown in Fig. 10. The concentration of Al and Cu was observed at the same position with the laser power of 1300 W. The formation of Ti₂(Cu,Al) observed in Fig. 6(e) was thus identified, which indicated that metallurgical bond at the intermediate zone was realized. At the seam head zone, Mg-Cu eutectic microstructure was also produced in large quantities at the laser power of 1300 and 1700 W, which was associated with the enhanced flow and vortex formed in the molten pool with the higher laser power as shown in Fig. 6(f) and (i), respectively.

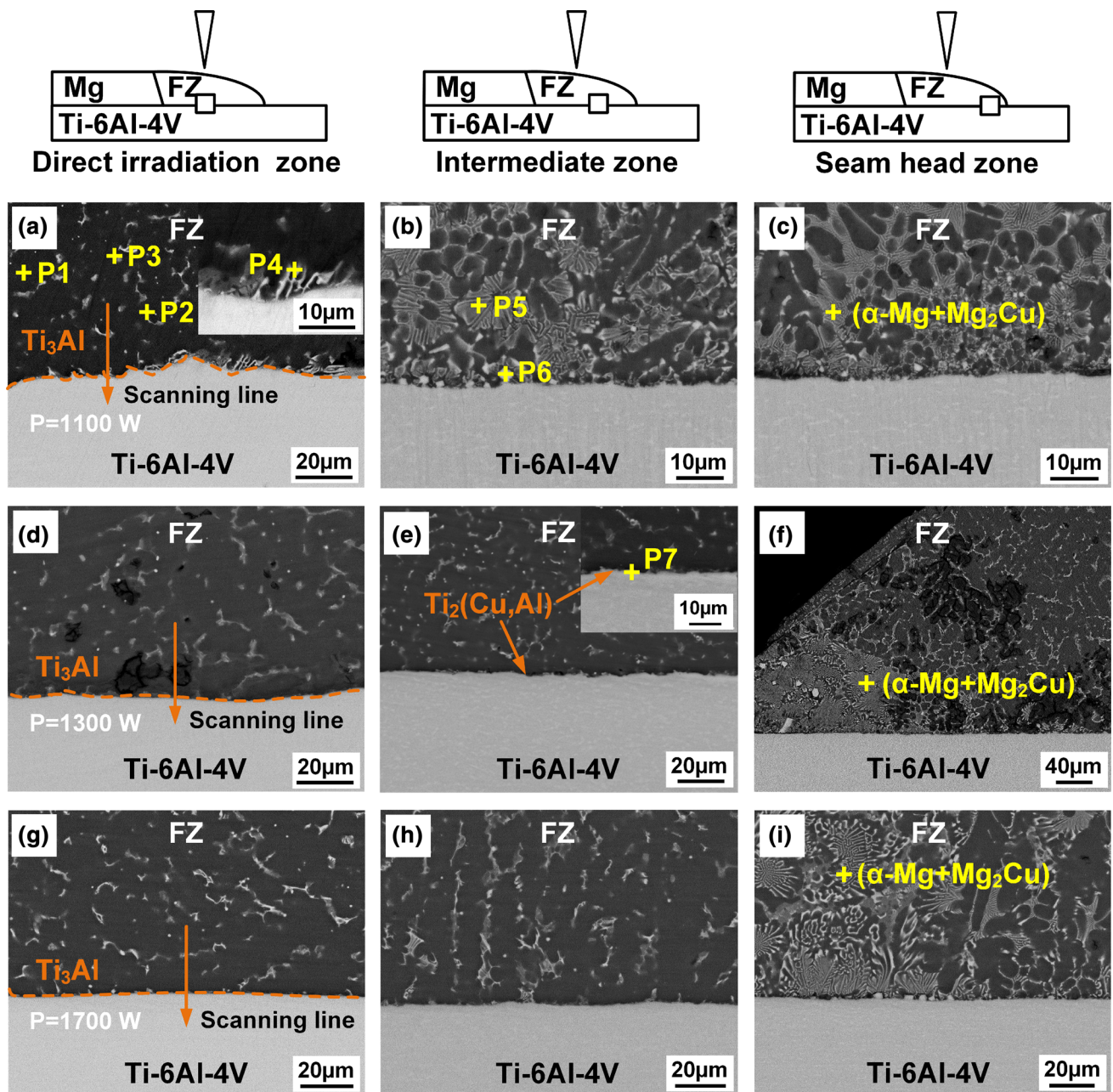


Fig. 6 Microstructure of laser welded-brazed Mg/Cu-coated Ti joints with the laser power of 1100, 1300 and 1700 W

Table 3 EDS analysis results of different zones in Fig. 6 and 15 (at.%)

Point	Mg	Al	Cu	Zn	Ti	Possible phases
1	96.58	3.42				α -Mg solid solution
2	82.03	17.08				$Mg_{17}Al_{12}$
3	76.62	20.40		2.70	...	$Mg_{17}(Al,Zn)_{12}$
4	80.37	13.22	6.41	α -Mg + Mg_2Cu
5	80.97	9.56	9.48	α -Mg + Mg_2Cu
6	34.82	22.18	42.23		...	$Mg(Al,Cu)_2$
7		10.09	20.37		68.46	$Ti_2(Cu, Al)$
8	0.23	24.65	5.34		68.78	Ti_3Al
9	6.63	23.72			69.65	Ti_3Al
10	83.68	11.24		1.98		$Mg_{17}Al_{12}$

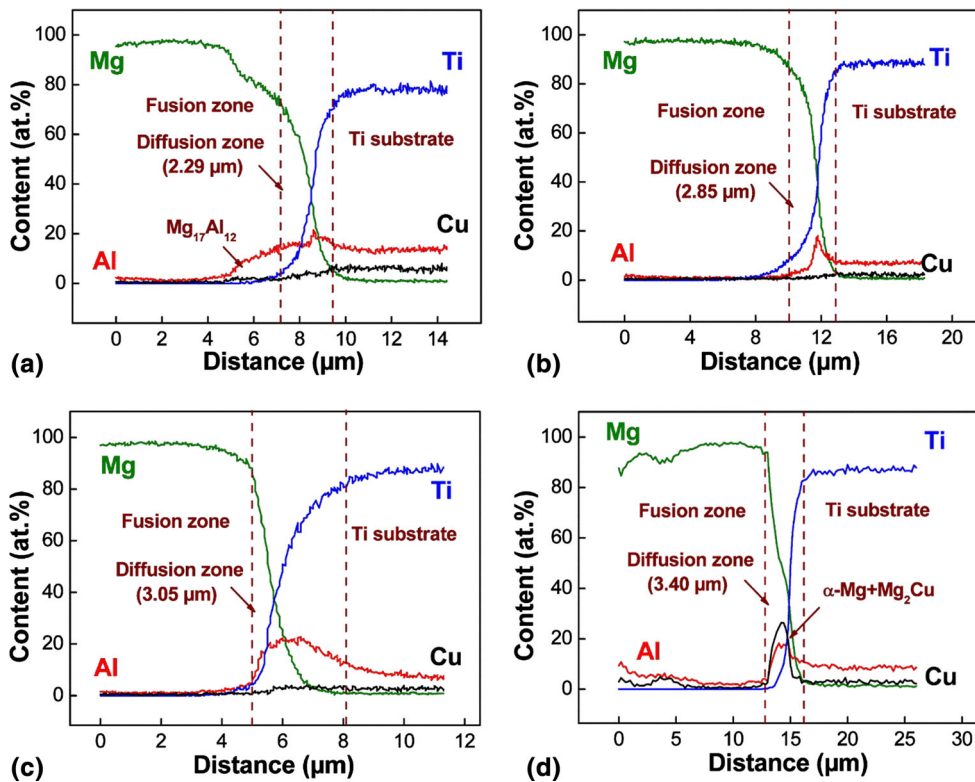


Fig. 7 Line scanning results of brazed interface for Mg/Ti joints at direct irradiation zone: (a) 1100 W, (b) 1300 W, (c) 1500 W, (d) 1700 W

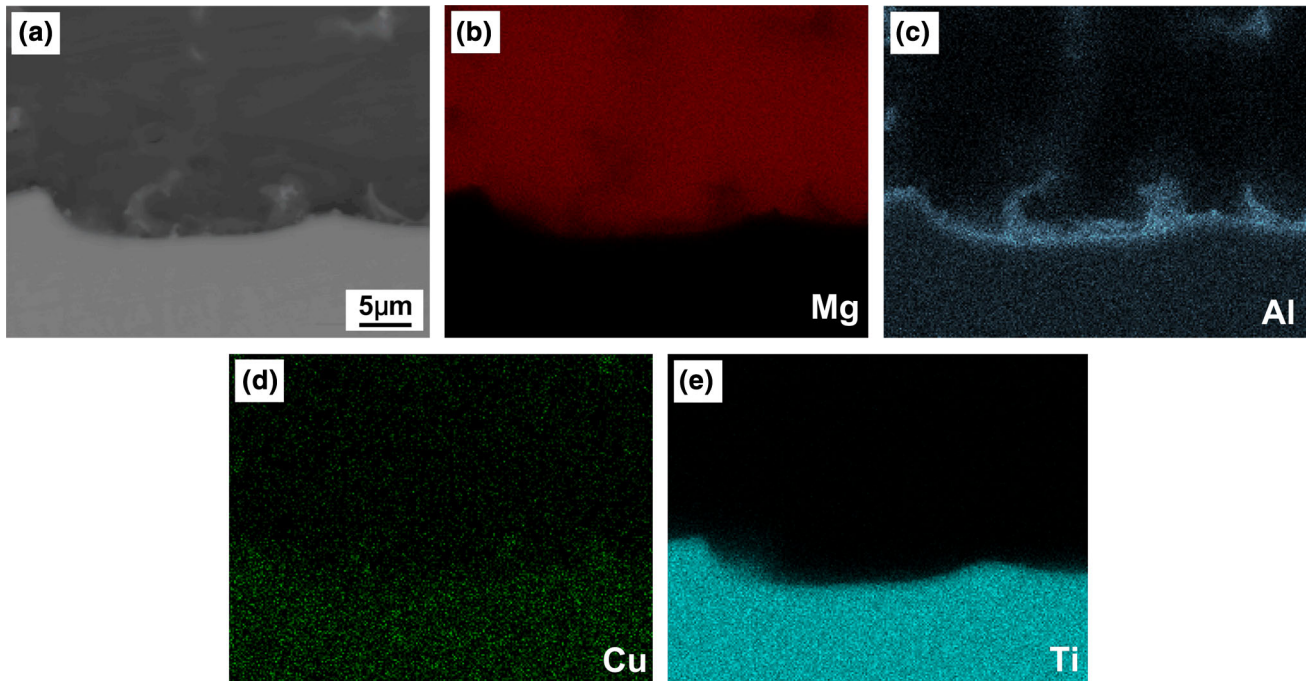


Fig. 8 Elemental distribution of Mg/Cu-coated Ti interface at direct irradiation zone with the laser power of 1300 W: (a) SEM micrograph of interfacial microstructure, (b)-(e) Mg, Al, Cu, Ti mapping

Micro-XRD analysis was also conducted to further verify the reaction products produced along the interface at the intermediate zone with the laser power of 1300 W. The result

shown in Fig. 11 confirmed that diffraction peaks of Ti_3Al , Mg_2Cu and $Ti_2(Cu,Al)$ phase were detected, which was in good agreement with the EDS analysis results obtained in Fig. 6(e).

3.3 Mechanical Properties

Figure 12 presents the hardness distribution across the Mg fusion zone/Ti joints obtained with various laser powers. The homogeneous distribution of hardness value was observed in the Mg fusion side with the average value of 74.4 HV. An obvious sharp increase in hardness value across the FZ/Ti was observed in all cases. Meanwhile, more distinct rise in hardness value was noticed in the case of higher laser power. It was because the interfacial reaction and atomic diffusion were accelerated as heat input increased, leading to the formation of more intermetallic compounds.

At the side of Ti base metal, the average hardness value was 374.8 HV. The increase in hardness values under the high power of 1500 and 1700 W was mainly attributed to more fusion of titanium alloy and atomic diffusion of Ti and Al, which was consistent with the observation in Fig. 7. Note that the inhomogeneity of joint hardness value reduced with enhancing heat input, which was associated with phase transformation in titanium alloy during the welding process of heating and cooling. In accordance with the report by Wei et al. (Ref 23), Al element would restrict phase transformation from α -Ti to β -Ti. Consequently, the amount of Al element diffused into Ti alloy increased with the increase in heat input.

The fracture load of Mg/Cu-coated Ti was evaluated, and results are shown in Fig. 13. The joint strength first presented up trend and then decreased after the laser power increased to more than 1300 W. The value of fracture load was 1855 N at the laser power of 1100 W. When the laser power further increased to 1300 W, maximum fracture load was obtained. The value attained 2314 N, reaching 85.7% joint efficiency relative to Mg base metal. The main reason for upward trend in fracture load as the laser power improved from 1100 W to 1300 W was that the appropriate heat input could increase weld penetration, joining area and wettability of molten filler on the Ti surface combined with the results of appearance and contact angle and seam width shown in Fig. 3 and 5. However, joint strength started to decrease with a further increase in laser power which caused excessive evaporation of filler presented in Fig. 3(d) and (e). This burn loss gave rise to weak interfacial bonding and thereafter reduced the fracture load. The fracture load of Mg/Cu-coated Ti joints obtained in previous works is

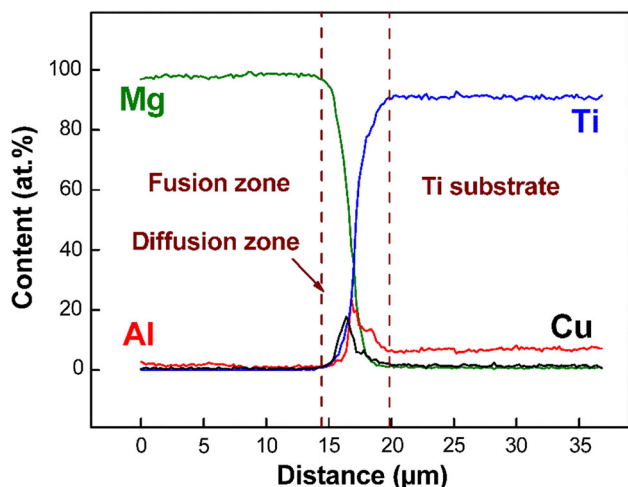


Fig. 9 Line scanning result of brazed interface for Mg/Cu-coated Ti joint at the intermediate zone with the laser power of 1300 W

presented in Fig. 13. The maximum value achieved in the present study was higher than the tensile-shear value obtained in previous reports when joining Mg to Ti (Ref 4, 9, 10). The fracture load increased by 12.3% when compared with that of Mg/non-coated Ti in our previous work (Ref 10). The highest tensile-shear load of joint with Cu coating was slightly lower than that with Ni coating (Ref 24).

All specimens produced with different laser powers fractured along the interface of Mg/Cu-coated Ti joints during the tensile-shear testing, as presented in Fig. 14(a). Based on the analysis of microstructure shown in Fig. 6, Ti_3Al reaction layer and some $Ti_2(Cu,Al)$ intermetallic compounds formed at the interface of direct irradiation zone (zone b in Fig. 14a) and intermediate zone (zone c in Fig. 14a). In order to clarify detailed position of crack along the interface, EDS mapping of fractured joint was conducted. Figure 14(b) shows the EDS mapping result of fracture location at zone b in Fig. 14(a) produced with the laser power of 1300 W. Al was concentrated and Mg was residual at the interface of Ti side, and Ti element was only observed at the Ti side, indicating that crack propagation developed along the interface between the Ti_3Al reaction layer and the FZ at this zone. The EDS mapping result of zone c is presented in Fig. 14(c). A small amount of Mg element and Cu element was found remaining at the Ti surface, and no Ti element was found on the Mg side, suggesting fracture occurred at the FZ adjacent to the $Ti_2(Cu,Al)$ side instead of reaction layer/Ti interface. Combined with microstructure shown in Fig. 6(e) and EDS mapping analysis result shown in Fig. 10, it could be concluded that $Ti_2(Cu,Al)$ enhanced the interfacial bonding of Mg/Cu-coated Ti in this work.

The fracture surfaces of the joints were observed after tensile-shear test and some differences were distinguished as shown in Fig. 15. For the joint welded at the laser power of 1100 W, the feature of fracture surface at the Ti side was characterized by smooth surface as shown in Fig. 15(a), which was indicative of inadequate interfacial reaction owing to lower energy input under this laser power. A large amount of oxides were observed near the joining zone arrowed in Fig. 15(a). The rupture was observed in some areas of Fig. 15(a). Some particles were observed on the magnified image of fracture surface, as shown in Fig. 15(b). Based on the EDS result, the particles mainly contained 24.65 at.% Al and 68.78 at.% Ti, which was confirmed as Ti_3Al phase. This result suggested that the weak metallurgical bonding at the interface was achieved by mutual diffusion of Al atoms and Ti atoms at the laser power of 1100 W, which gave rise to the smooth fracture surface for the most part in Fig. 15(a). However, fracture surfaces were characterized by tear ridge for joints made at the laser power of 1300 and 1700 W (Fig. 15c and e), implying the interface had high resistance to the crack propagation. Compared with the surface in Fig. 15(b), a great number of particles with residual Mg were found to exist at the fracture surface as seen at higher magnification of Fig. 15(c). These dispersed particles at the Ti side was also identified as Ti_3Al phase since it mainly consisted of 21.8 at.% Al and 68.06 at.% Ti, according to EDS result of P9 shown in Fig. 15(d). Meanwhile, EDS result indicated that scraggly part at P10 was composed of 83.68 at.% Mg, 11.24 at.% Al and 1.98 at.% Zn, suggesting it was residual α -Mg attached to the Ti side after tensile-shear test. The phase identification indicated the fracture occurred at the Ti_3Al reaction layer/the FZ interface at direct irradiation zone, which was consistent with the observation in Fig. 14(b). Obvious tear

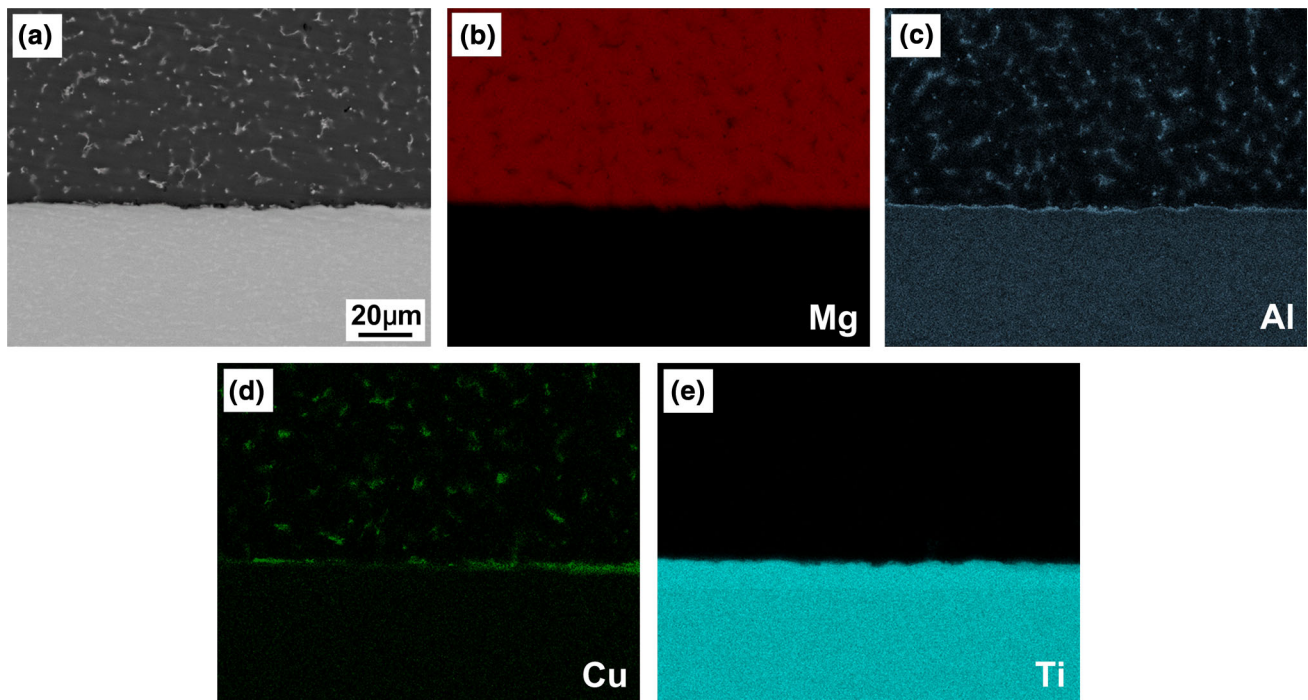


Fig. 10 Elemental distribution of Mg/Cu-coated Ti interface at the intermediate zone with the laser power of 1300 W: (a) SEM micrograph of interfacial microstructure, (b)-(e) Mg, Al, Cu, Ti mapping

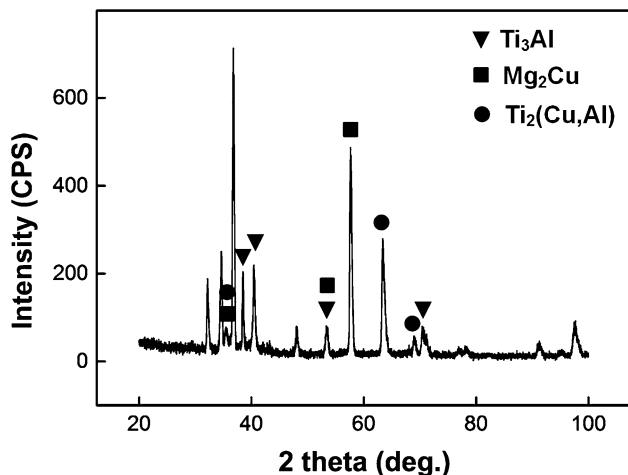


Fig. 11 Micro-XRD pattern of fusion zone/Ti interface at the intermediate zone produced with the laser power of 1300 W

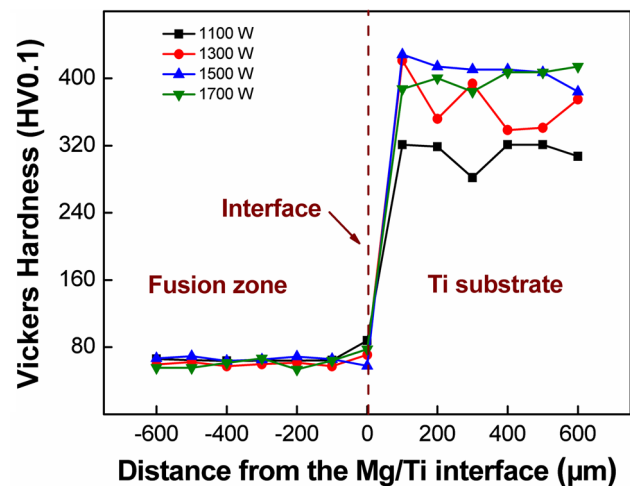


Fig. 12 Hardness distribution across the brazed interface of Mg/Cu-coated Ti joints

ridge and Ti_3Al particles observed with the increase in laser power indicated atomic diffusion was accelerated with more heat input resulting in the enhanced interfacial reaction and metallurgical joining at direct irradiation zone, which determined the joint strength.

3.4 Joining Mechanism of Mg to Cu-Coated Ti

According to the work and results above, a schematic diagram describing interfacial reaction mechanism of Mg to Ti is shown in Fig. 16. Firstly, laser beam irradiated on Mg filler metal and it first melted. Molten Mg-based filler then dropped on Cu coating layer and spread out (Fig. 16a). Cu coating dissolved immediately in the effect of laser irradiation and heat

conducted by Mg molten metal. Whereafter, Cu coating totally melted and Cu atoms were involved into molten filler metal (Fig. 16b). At the intermediate zone, a portion of molten Cu coating still adhered to the interface owing to weaker stirring in molten pool. As the welding continued, the Ti surface was indirect contact with molten filler at direct irradiation zone. Al atoms contained in Mg-based filler dissolved into Ti substrate. Meanwhile, high temperature made Ti become active and diffused into Mg liquid (Fig. 16c). As the diffusion progressed, Al atoms and Ti atoms continually gathered together at the liquid/solid interface. The diffusion distance was relatively short with the characteristics of rapid heating and cooling rate of laser process. At the intermediate zone, Cu atoms gradually

diffused from the Mg/Ti interface to the liquid mixed metal. Upon cooling stage, Ti_3Al was precipitated firstly along the interface as the temperature decreased to 1180 °C (Fig. 16d), which was referred by Al-Ti binary phase diagram. With the temperature decreased to 650 °C and below, the liquid filler began to solidify. Meanwhile, Al atoms, Cu atoms and Ti atoms reacted and then formed $Ti_2(Cu,Al)$ phase at the interface at the intermediate zone. Finally, a large amount of Mg-Cu eutectic structures formed at the FZ close to the interface due to the diffusion of part Cu element as shown in Fig. 16(e).

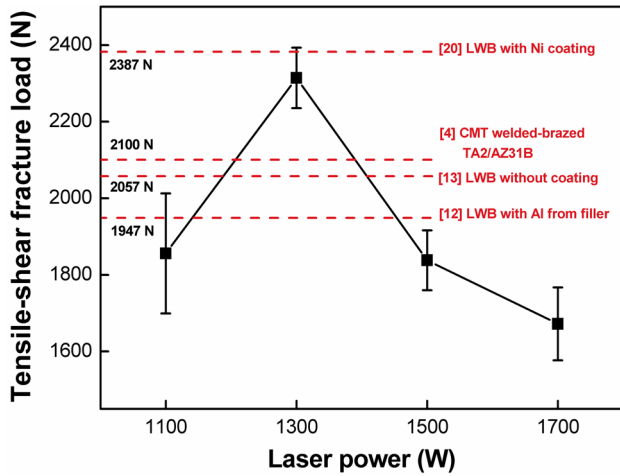


Fig. 13 Tensile-shear strength of laser welded-brazed Mg/Cu-coated Ti joints vs. laser power

structures formed at the FZ close to the interface due to the diffusion of part Cu element as shown in Fig. 16(e).

4. Conclusions

The influence of laser power on the interfacial microstructure and mechanical properties of dissimilar joint of laser welded-brazed Mg/Cu-coated Ti was investigated. The bonding mechanism was clarified based on the above results. The conclusions were drawn as follows:

1. Laser welding-brazing of AZ31B magnesium alloy to Cu-coated Ti-6Al-4V titanium alloy has been joined successfully with AZ92 Mg-based filler. Increasing laser power contributed to improvement of wetting-spreading ability of molten filler on Cu-coated Ti surface. In this case, uniform bead without obvious defect was produced under the laser power of 1300 W-1500 W, while burning loss defect occurred when the laser power further increased.
2. Ti_3Al phase was produced at the direct irradiation zone, and the diffusion distance of Al atoms and Ti atoms varied little with the increase in laser power. A small amount of $Ti_2(Cu,Al)$ interfacial compound formed at the intermediate zone. The distribution of (α -Mg + Mg_2Cu) eutectic structures was more dispersive in the weld seam with the increase in heat input caused by the enhanced flow and vortex.

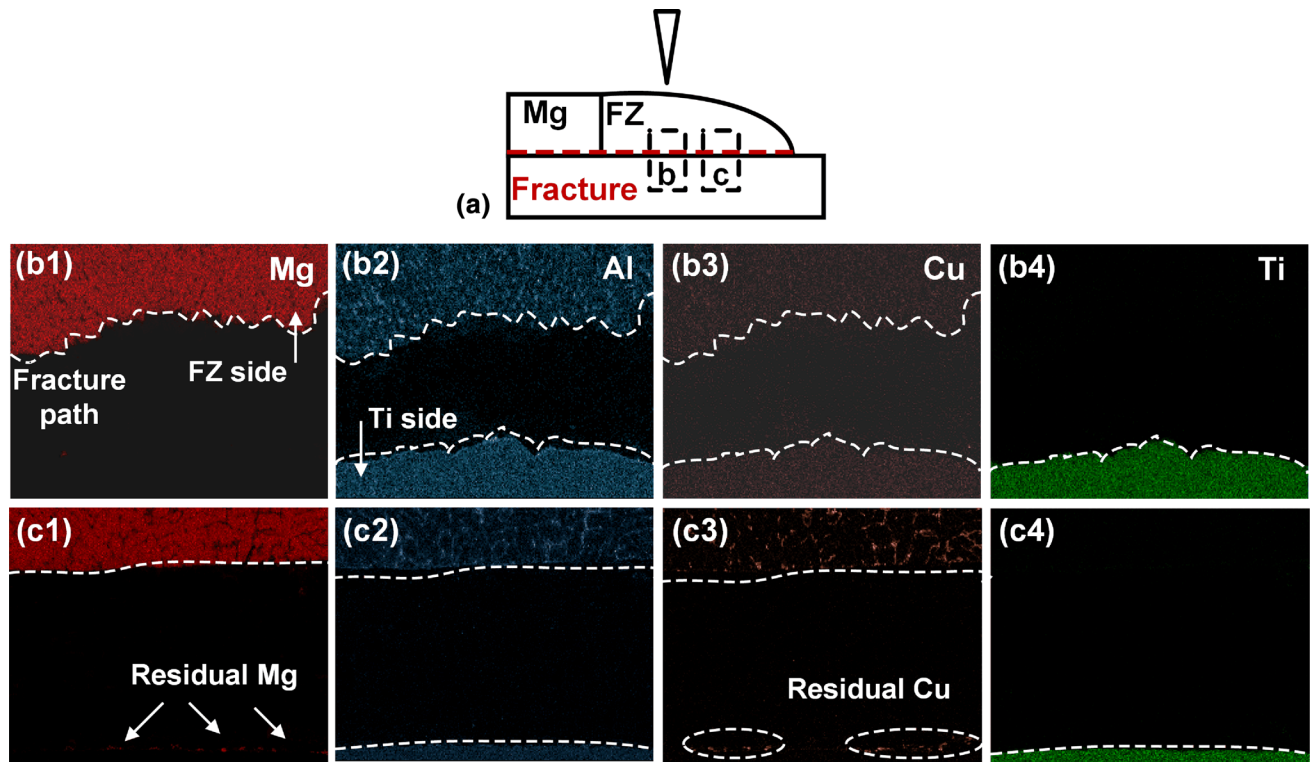


Fig. 14 Fracture path of Mg/Cu-coated Ti joint produced with the laser power of 1300 W: (a) the schematic of fracture path and observation location; (b1)-(b4) Mg, Al, Cu, Ti mapping of zone b, (c1)-(c4) Mg, Al, Cu, Ti mapping of zone c

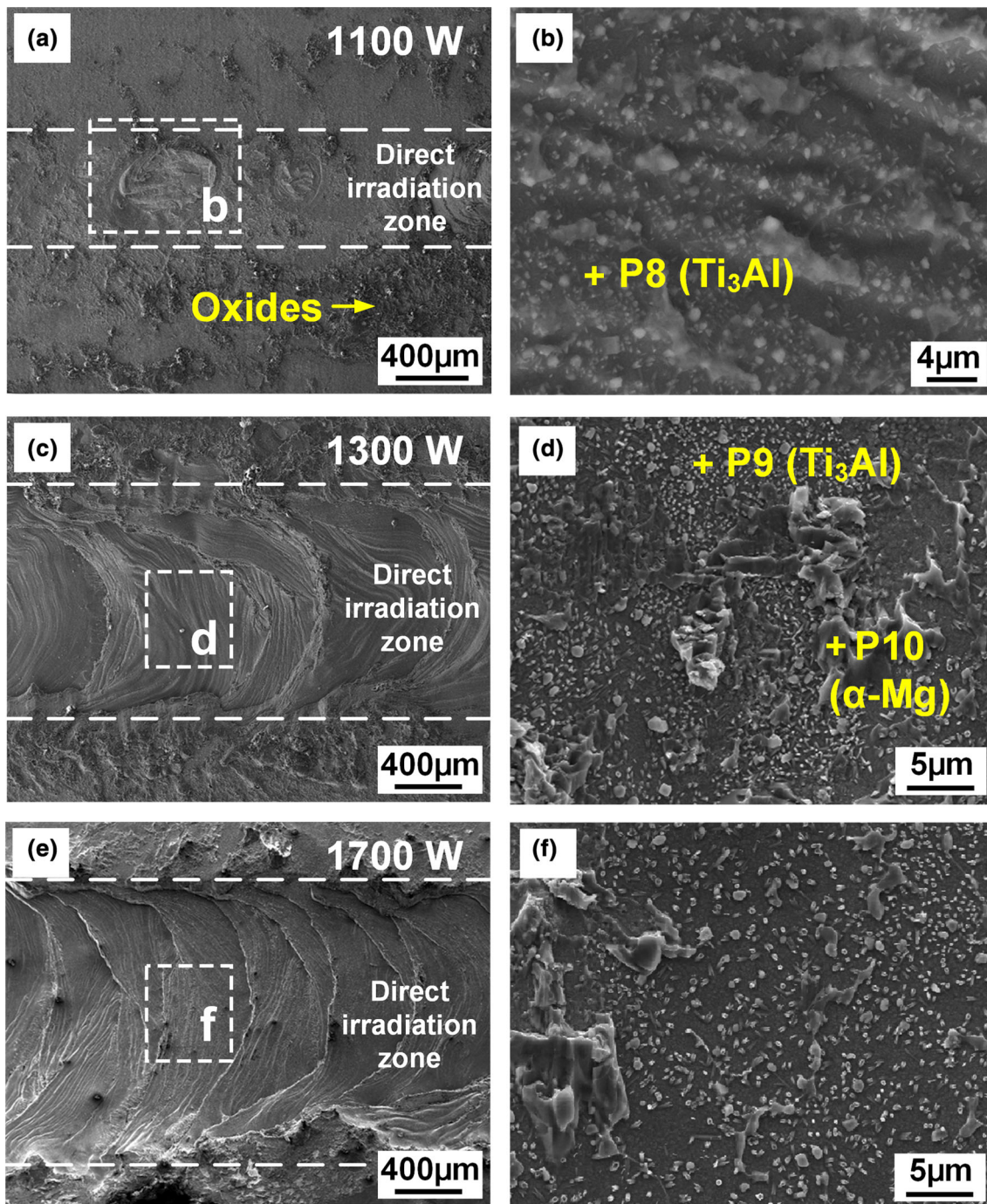


Fig. 15 Fracture surface morphologies of Mg/Cu-coated Ti joints at different laser powers: (a) laser power 1100 W, (b) higher magnification of Zone b, (c) laser power 1300 W, (d) higher magnification of Zone d, (e) laser power 1700 W, (f) higher magnification of Zone f

3. The maximum fracture load of the joint reached 2314 N with the laser power of 1300 W, representing 85.7% joint efficiency relative to Mg base metal. The fracture mode of all joints was interfacial failure. The crack propagation developed along the Ti_3Al / the fusion zone interface at

the direct irradiation zone and occurred at the fusion zone close to the $Ti_2(Cu,Al)$ side at the intermediate zone, respectively.

4. Fracture surface obtained with the laser power of 1100 W presented, for the most part, smooth characteris-

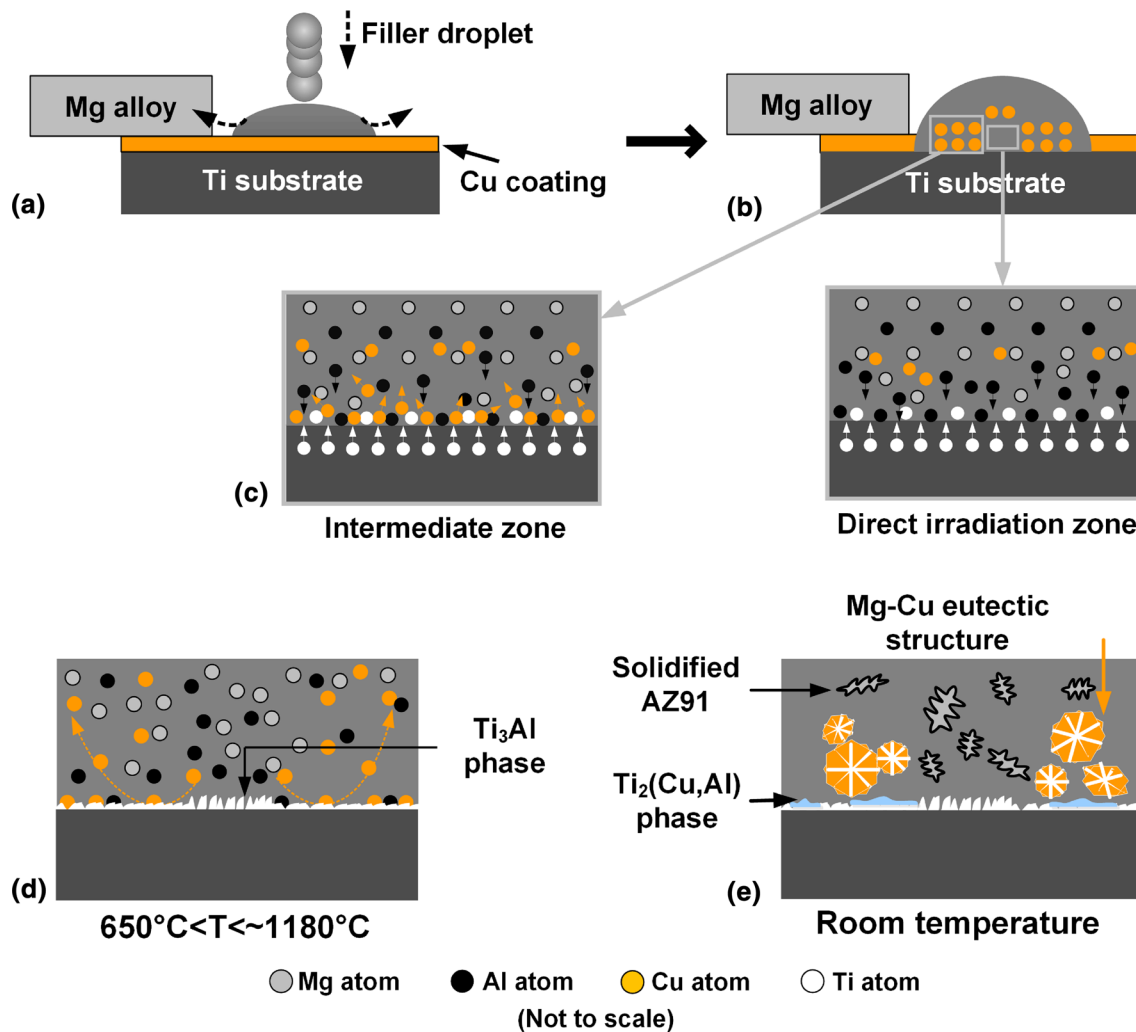


Fig. 16 Schematic of joining mechanism: (a), (b) melting of filler and Cu coating, (c) dissolution and diffusion of Al atoms, Cu atoms at the intermediate zone, and Al atoms, Ti atoms at the direct irradiation zone, (d), (e) solidification of interfacial zone at different temperature ranges

tic. Obvious tear ridge was observed with the increase in laser power, suggesting that it could prevent crack propagation effectively and thus enhanced mechanical properties of the joint.

Acknowledgments

The study was financially supported by National Natural Science Foundation of China (Grant No. 51504074), Key Research and Development Program of Shandong Province (Grant Nos. 2017GGX30147 and 2017CXGC0811), China Postdoctoral Science Foundation (Grant Nos. 2015M571406 and 2016T90280).

References

1. M. Aonuma and K. Nakata, Effect of Alloying Elements on Interface Microstructure of Mg-Al-Zn Magnesium Alloys and Titanium Joint by Friction Stir Welding, *Mater. Sci. Eng., B*, 2009, **161**(1), p 46–49
2. M. Aonuma and K. Nakata, Effect of Calcium on Intermetallic Compound Layer at Interface of Calcium Added Magnesium-Aluminum Alloy and Titanium Joint by Friction Stir Welding, *Mater. Sci. Eng., B*, 2010, **173**(1–3), p 135–138
3. C. Xu, G. Sheng, H. Wang et al., Reinforcement of Mg/Ti Joints Using Ultrasonic Assisted Tungsten Inert Gas Welding-Brazing Technology, *Sci. Technol. Weld. Join.*, 2014, **19**(8), p 703–707
4. R. Cao, T. Wang, C. Wang et al., Cold Metal Transfer Welding-Brazing of Pure Titanium TA2 to Magnesium Alloy AZ31B, *J. Alloy. Compd.*, 2014, **605**(14), p 12–20
5. A.M. Atieh and T.I. Khan, Effect of Process Parameters on Semi-Solid TLP Bonding of Ti-6Al-4V to Mg-AZ31, *J. Mater. Sci.*, 2013, **48**(19), p 6737–6745
6. A.M. Atieh and T.I. Khan, Application of Ni and Cu Nanoparticles in Transient Liquid Phase (TLP) Bonding of Ti-6Al-4V and Mg-AZ31 Alloys, *J. Mater. Sci.*, 2014, **49**(22), p 7648–7658
7. A.M. Atieh and T.I. Khan, TLP Bonding of Ti-6Al-4V and Mg-AZ31 Alloys Using Pure Ni Electro-Deposited Coats, *J. Mater. Process. Technol.*, 2014, **214**(12), p 3158–3168
8. M. Gao, Z.M. Wang, X.Y. Li et al., Laser Keyhole Welding of Dissimilar Ti-6Al-4V Titanium Alloy to AZ31B Magnesium Alloy, *Metall. Mat. Trans. A*, 2012, **43**(1), p 163–172
9. C. Tan, X. Song, B. Chen et al., Enhanced Interfacial Reaction and Mechanical Properties of Laser Welded-Brazed Mg/Ti Joints with Al Element from Filler, *Mater. Lett.*, 2016, **167**, p 38–42
10. C. Tan, B. Chen, S. Meng et al., Microstructure and Mechanical Properties of Laser Welded-Brazed Mg/Ti Joints with AZ91 Mg Based Filler, *Mater. Des.*, 2016, **99**, p 127–134
11. C. Dharmendra, K.P. Rao, J. Wilden et al., Study on Laser Welding-Brazing of Zinc Coated Steel to Aluminum Alloy with a Zinc Based Filler, *Mater. Sci. Eng. A*, 2011, **528**, p 1497–1503

12. S. Chen, Z. Zhai, J. Huang et al., Interface Microstructure and Fracture Behavior of Single/Dual-Beam Laser Welded Steel-Al Dissimilar Joint Produced with Copper Interlayer, *Int. J. Adv. Manuf. Technol.*, 2016, **82**(1), p 631–643
13. S. Chen, J. Huang, K. Ma et al., Microstructures and Mechanical Properties of Laser Penetration Welding Joint With/Without Ni-Foil in an Overlap Steel-on-Aluminum Configuration, *Metall. Mater. Trans. A*, 2014, **45**(7), p 3064–3073
14. Y. Chen, S. Chen, and L. Li, Effects of Heat Input on Microstructure and Mechanical Property of Al/Ti Joints by Rectangular Spot Laser Welding-Brazing Method, *Int. J. Adv. Manuf. Technol.*, 2009, **44**(3), p 265–272
15. L. Li, C. Tan, Y. Chen et al., Comparative Study on Microstructure and Mechanical Properties of Laser Welded-Brazed Mg/Mild Steel and Mg/Stainless Steel Joints, *Mater. Des.*, 2013, **43**(43), p 59–65
16. J. Miettinen, Thermodynamic Description of Cu–Mg–Ni and Cu–Mg–Zn Systems, *CALPHAD*, 2008, **32**(2), p 389–398
17. M.A. Turchanin, P.G. Agraval, and A.R. Abdulov, Thermodynamic Assessment of the Cu-Ti-Zr System I, Cu-Ti System, *Powder. Metall. Met. C+*, 2008, **47**(5–6), p 344–360
18. C. Tan, X. Song, S. Meng et al., Laser Welding-Brazing of Mg to Stainless Steel: Joining Characteristics, Interfacial Microstructure, Mechanical Properties, *Int. J. Adv. Manuf. Technol.*, 2016, **86**(1), p 1–11
19. C. Xu, G. Sheng, H. Wang et al., Tungsten Inert Gas Welding-Brazing of AZ31B Magnesium Alloy to TC4 Titanium Alloy, *J. Mater. Sci. Technol.*, 2015, **32**(2), p 167–171
20. M. Gao, Z.M. Wang, J. Yan et al., Dissimilar Ti/Mg Alloy Butt Welding by Fiber Laser with Mg Filler Wire—Preliminary Study, *Sci. Technol. Weld. Join.*, 2011, **16**(6), p 488–496
21. L. Ma, D. He, X. Li et al., Characterization of High-Frequency Induction Brazed Magnesium Alloy Joint with an Al-Mg-Zn Filler Metal, *J. Mater. Eng. Perform.*, 2011, **20**(2), p 219–222
22. C. Tan, W. He, X. Gong et al., Influence of Laser Power on Microstructure and Mechanical Properties of Fiber Laser-Tungsten Inert Gas Hybrid Welded Mg/Cu Dissimilar Joints, *Mater. Des.*, 2015, **78**, p 51–62
23. S. Wei, Y. Li, J. Wang et al., Microstructure and Joining Mechanism of Ti/Al Dissimilar Joint by Pulsed Gas Metal Arc Welding, *Int. J. Adv. Manuf. Technol.*, 2014, **70**(5), p 1137–1142
24. C. Tan, Q. Lu, B. Chen et al., Influence of Laser Power on Microstructure and Mechanical Properties of Laser Welded-Brazed Mg to Ni Coated Ti Alloys, *Opt. Laser Technol.*, 2017, **89**, p 156–167